Materials and Design 55 (2014) 85–92

Contents lists available at ScienceDirect

Materials and Design

journal homepage: www.elsevier.com/locate/matdes

Structure–fracture properties relationship for Polypropylene reinforced with fly ash with and without maleic anhydride functionalized isotactic Polypropylene as coupling agent

Esteban Igarza [a], Santiago García Pardo [b,c], María José Abad [b], Jesús Cano [b], María José Galante [d], Valeria Pettarin [e], Celina Bernal [a,*]

[a] Instituto de Tecnología en Polímeros y Nanotecnología ITPN (UBA-CONICET), Facultad de Ingeniería, Universidad de Buenos Aires, Av. Las Heras 2214, C1127AAQ Buenos Aires, Argentina
[b] Grupo de Polímeros, Departamento de Física, E.U.P.-Ferrol, Universidad de A Coruña, Avda. 19 febrero, s/n, 15405 Ferrol, Spain
[c] Centro Galego do Plástico (CGaP), A Cabana s/n, 15590 Ferrol, Spain
[d] Grupo de Polímeros Nanoestructurados, INTEMA (UNMdP-CONICET), Departamento de Ingeniería en Materiales, Universidad Nacional de Mar del Plata, J.B. Justo 4302, B7608FDQ Mar del Plata, Argentina
[e] Grupo de Ciencia e Ingeniería de Polímeros, INTEMA (UNMdP-CONICET), Departamento de Ingeniería en Materiales, Universidad Nacional de Mar del Plata, J.B. Justo 4302, B7608FDQ Mar del Plata, Argentina

ARTICLE INFO

Article history:
Received 19 March 2013
Accepted 15 September 2013
Available online 2 October 2013

Keywords:
Deformation behavior
Fracture
Polymer composites
Poly(propylene)
Fly ash

ABSTRACT

The deformation and fracture behavior of PP/ash composites with and without maleic anhydride functionalized iPP (MAPP) as coupling agent was investigated, focusing on the effect of ash content and loading conditions. A decreasing trend of tensile strength and strain at break values with filler content was observed for unmodified composites, whereas these properties were roughly independent of ash content for the composites with MAPP. In quasi-static fracture tests, all materials displayed ductile behavior. Most composites exhibited improved fracture properties with respect to the matrix as a result of the toughening mechanisms induced by the ash particles. Under impact loading conditions, in contrast, all materials displayed fully brittle behavior. Impact critical fracture energy values of the composites were higher than those of PP and they also presented a maximum which was explained in terms of the comprehensive analysis of the crystallinity development in PP. The incorporation of MAPP led to better dispersion of ash particles in the matrix but was detrimental to the material fracture behavior independently of loading conditions. Increased interfacial adhesion promoted by MAPP hindered particle-induced toughening mechanisms.

1. Introduction

The most commonly used thermoplastics in industry are polyolefins. Among them, a useful commodity polymer with outstanding properties is poly(propylene) (PP). It is characterized for having low density, sterilizability, good surface hardness, very good abrasion resistance, excellent electrical properties, as well as good mechanical and barrier properties to water. It also has low cost, worldwide production, simplicity of processing, capability to burn without producing toxic emissions, working security, and recyclability [1,2]. PP and its blends and composites find wide applications in automotive parts, extruded profiles, packaging, etc. However, there are some limitations and disadvantages that lead to the different modifications of the main material. The PP random copolymer (rPP) is one of the many modifications of neat Polypropylene which has been widely successfully adopted by industry. Frequently, PP is copolymerized with ethylene obtaining a copolymer which properties are mainly determined by the ethylene content. Ethylene units attach to the main polymeric chain of PP and are partially included in the crystalline phase of the material and hence, increase the amorphous phase of PP. The small amount of ethylene on rPP retains the stiffness and strength of neat Polypropylene but also improves its mechanical properties at low temperatures [3].

In structural and semi-structural applications of materials, in addition to high stiffness and mechanical strength, adequate fracture toughness is often required. In order to optimize these properties, the knowledge of the relationship between morphology and deformation behavior seems to be essential.

* Corresponding author.
E-mail addresses: labpolim@udc.es (S.G. Pardo), galant@fi.mdp.edu.ar (M.J. Galante), vpettarin@hotmail.com (V. Pettarin), cbernal@fi.uba.ar (C. Bernal).

0261-3069/$ - see front matter © 2013 Elsevier Ltd. All rights reserved.
http://dx.doi.org/10.1016/j.matdes.2013.09.055

A commonly used practice in industry to obtain new plastics with improved properties at relatively low cost is the incorporation of inorganic fillers into polymers [4]. In particular, the dispersion of organically modified layered silicates in PP has been found that lead to enhancement. Different polymer/clay nanocomposites have been successfully obtained based on several polymeric systems such as polyamide, epoxy, polyimide, polyurethane, Polypropylene, and polystyrene [2,5]. In the last decade nanocomposites based on thermoplastics modified with nanoclays emerged as a topic of industrial and academic interest [6–8]. These nanocomposites have been reported to exhibit visible improvements in mechanical properties, flame resistance and barrier properties when compared with the corresponding raw materials and micro- and macro-composites [9]. However, it has been claimed that only well-dispersed and well exfoliated nanoparticles can lead to the expected improvement of properties [10].

In addition, there is an increasing trend of current industries to re-use their wastes, mainly as a result of economic and ecological concerns.

Ashes are solid industrial wastes produced in the combustion of carbon and other fossil fuels. They are generally composed of a significant amount of SiO_2 and lower contents of Al_2O_3, Fe_2O_3, Na_2O, MgO, K_2O, etc. They are cheaper and more environmentally friendly than conventional mineral fillers, thus they represent an appealing alternative as reinforcement in polymers.

The use of ash as reinforcement in polymer composites has been already the subject of many investigations and several authors have used fly ash as filled reinforcing material in Polypropylene and its blends. They generally found that the incorporation of ash into PP led to stiffer but also more brittle and weaker materials [11]. Nevertheless, only a few studies have been reported concerning the fracture behavior of thermoplastic composites reinforced with ashes from biomass origin [12–14]. In these works, the effect of different silane-type coupling agents on the materiaĺs fracture response was investigated.

Furthermore, it is well known [15,16] that the macroscopical behavior of heterogeneous materials depends on many factors such as composition, behavior of each component, geometrical arrangement of the phases, and interfacial properties.

Interfacial adhesion between inorganic fillers and polymers is often rather poor. Therefore, different additives able to react with the filler are frequently added in the formulations. They have reactive groups compatible with the chemical nature of the polymer and the filler [17,18]. The addition of coupling agents, has been demonstrated to improve interfacial adhesion between the filler and the polymer matrix and hence, to be beneficial to some important material properties.

It is well established in the literature [19] that the interfacial shear strength between glass and polyolefins is very low, as a result wetting is poor and shrinkage during crystallization also contributes to this lack of wetting. Moreover, the surface roughness of glass does not offer sites for mechanical anchoring. Interfacial adhesion has been successfully improved in this case by using polymeric coupling agents such as grafted polyolefins. It has been recently reported in the literature that simultaneous improvements in tensile strength, Young's modulus and elongation at break were obtained by using maleic anhydride grafted High Density Polyethylene (HDPE) as compatibilizer in HDPE/rice husk ash composites [20].

In this work, the deformation and fracture behavior of PP/ash composites with and without maleic anhydride functionalized iPP (MAPP) as coupling agent was investigated, focusing on the effect of ash content and loading conditions (quasistatic *versus* dynamic loading). In addition, crystallization behavior of the different PP composites was also evaluated and their influence over the mechanical response analyzed.

2. Experimental details

2.1. Materials

Fly ashes obtained from biomass combustion (kindly supplied by Industrias del Tablero S.A. (INTASA), Galicia, Spain) were used as composites reinforcement. They were separated using a sieve of mesh 400 μm. Particle size distribution determined from SEM micrographs of ash particles has been reported in a previous paper (mean diameter of 30.88 ± 16.42 μm) [12].

The thermoplastic matrix was an isotactic Polypropylene (PP 070G2 M) delivered by Repsol-YPF, with a melt flow index of 12 g/10 min (230 °C, 2.16 kg) and a density of 0.902 g/cm^3. A commercially available polymer processing additive (Dynamar FX 5911, Dyneon, 3M Company) was used in order to improve processing and allow using high viscosity formulations. The blend of PP and the processing additive will be referred to in this work as the PP matrix.

Maleic anhydride functionalized iPP (MAPP) (Fusabond® MD 511 D, Dupont) at 1 wt% respect to the weight of PP was incorporated into the filler as coupling agent.

2.2. Sample preparation

Different contents of ash (10, 20 and 30 wt%) and Polypropylene were mixed in a single screw extruder (Brabender DSE20) at 220 °C and 30 r.p.m.

Granules of PP and the composites were compression-molded into 3 and 8 mm plaques at 200 °C, under a pressure of 10 bar for 10 min followed by 50 bar for 20 min. Then, the plaques were rapidly cooled down by circulating water within the press plates under a pressure of 50 bar for 25 min. Thermal stresses generated during molding were released by annealing the plaques in an oven at 100 °C for 3 h.

2.3. Mechanical characterization

Uniaxial tensile tests were performed on dog-bone specimens (thickness, B = 3 mm) in an Instron dynamometer 4467 at 5 mm/min in accordance with ASTM: D638-03 standard recommendations. True stress–strain curves were obtained from these tests by dividing load values by the actual area at each instant assuming constant volume during deformation. Young's modulus, tensile strength and ultimate strain values were determined from these curves. A minimum of four specimens were tested for each system, the average values of the mechanical parameters and their deviations were reported.

Fracture characterization was carried out on single-edge notched bend (SENB) specimens cut out from compression-molded thick plaques (thickness, B = 8 mm). Sharp notches were introduced by sliding a fresh razor blade into a machined slot. Crack-to-depth (a/W), thickness-to-depth (B/W) and span-to-depth (S/W) ratios were always kept equal to 0.5, 0.5 and 4, respectively.

Quasi-static three-point-bending tests were performed in an Instron dynamometer 4467 at 1 mm/min. Critical stress intensity factor (K_{IQ}) and energy release rate (G_{IQ}) values at initiation were calculated from the maximum in the load–displacement curves by following ASTM: D5045-93 standard recommendations.

Impact fracture tests were also performed on SENB samples in an instrumented falling weight Factovis (Ceast, Italy) at a testing speed of 1 m/s. Critical impact energy release rate (G_{IC}) values were determined from these tests in accordance with ISO 17281 standard recommendations [21].

2.4. Fracture surface analysis

The fracture surfaces of SENB specimens tested in fracture tests under both quasi-static and impact loading conditions were examined using a JEOL JSM-6460LV scanning electron microscope (SEM) at an accelerating voltage of 20 kV. Samples were sputter coated with a thin layer of gold before they were observed.

2.5. Thermal analysis

Differential scanning calorimetry (DSC) analysis was performed using a DSC Pyris 1-(Perkin Elmer) under dry nitrogen atmosphere, in a temperature range from 30 to 210 °C. Prior to DSC recording, samples were heated to and kept at 210 °C for 5 min to erase the influence of any previous thermal history. Then, they were cooled at a rate of 10 °C min^{-1} to room temperature and subsequently heated from 30 to 210 °C at a heating rate of 10 °C min^{-1}. The crystallization temperature (T_c) and the enthalpy of crystallization (ΔH_c) were calculated from the cooling scans. The melting temperature (T_m) and the heat of melting (ΔH_m) were measured in the last scan. The crystallinity degree (x_c) was calculated as:

$$x_c = \frac{\Delta H}{(1-\phi)\Delta H^0} \quad (1)$$

where ΔH is the apparent enthalpy of fusion per gram of composite, ΔH^0 is the heat of fusion of a 100% crystalline PP which is of 207.1 kJ/kg [22], and ϕ is the weight fraction of ash.

2.6. X-ray diffraction

X-ray diffraction (XRD) analysis was performed on samples surface using a Phillips X'PERT MPD diffractometer (Cu Kα radiation λ = 1.5418 Å, generator voltage = 40 kV, current = 40 mA). Measurements were recorded every 0.02° θ steps for 1 s, each varying 2θ from 20° to 40°.

3. Results and discussion

3.1. Deformation behavior

Fig. 1a and b shows typical true stress–strain curves for the PP matrix and the composites with different ash content without and with MAPP as coupling agent, respectively. It can be observed in this figure, that all composites exhibited semiductile tensile behavior displaying some amount of plastic deformation after maximum stress (yield point). For the composites without coupling agent, the amount of plastic deformation was found to decrease as the ash content increased. Composites samples containing MAPP, on the other hand, failed almost immediately after the maximum or even at this point, showing no significant effect of ash content.

Macroscopically, broken samples did not exhibit significant stress whitening nor necking in agreement with the observed stress–strain curves behavior.

The addition of ash to PP led to an increase in stiffness (Table 1) as expected from the incorporation of a much stiffer second phase [15,16], whereas a significant reduction in both tensile strength and strain at break values (Table 1) was observed, probably as a result of the debonding of ash particles from the PP matrix [23]. Similar results have been reported in a previous paper [12].

In addition, the incorporation of MAPP in the composites formulation led to a slight increase in stiffness, suggesting better dispersion of ash particles in the PP matrix. Furthermore, tensile strength and elongation at break for the PP/MAPP/ash composites exhibited a significant change in their behavior as they were roughly independent of ash content. While tensile strength maintained a relatively high value within the composition range investigated, elongation at break greatly decreased for 10 wt% ash and limited ductility was observed for all composites independently of filler loading.

A negative effect from the addition of MAPP on the elongation at break has been previously reported by others [24] and explained in terms of a greater interaction between filler and matrix. This improved adhesion, facilitates the transfer of properties between the two materials. Therefore, rigid particles which are unable to deform hinder composites elongation, making them less ductile.

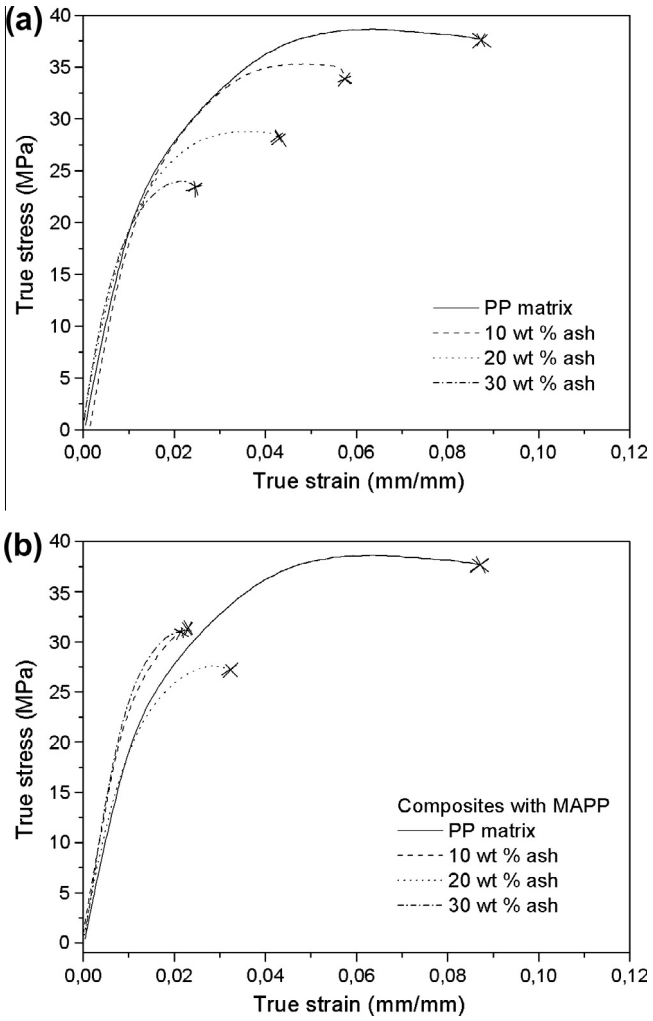

Fig. 1. Typical true stress–strain curves for the PP matrix and the different composites investigated. (a) Composites without MAPP. (b) Composites with MAPP.

Table 1
Tensile parameters for the different composites investigated.

Ash content (wt%)	Young's modulus, E (MPa)	Tensile strength, σ_u (MPa)	Strain at break, ε_b (mm/mm)
PP/ash composites			
0	1961.95 ± 23.30	39.54 ± 0.83	0.08 ± 0.01
10	2115.22 ± 183.66	35.05 ± 2.06	0.07 ± 0.01
20	2222.56 ± 113.09	28.83 ± 0.70	0.04 ± 0.01
30	2449.56 ± 91.55	24.27 ± 1.22	0.03 ± 0.01
PP/MAPP/ash composites			
10	2374.01 ± 288.58	31.19 ± 1.28	0.02 ± 0.01
20	2275.81 ± 35.61	28.26 ± 0.48	0.04 ± 0.01
30	2725.22 ± 38.64	30.68 ± 2.17	0.02 ± 0.01

In our composites, the reduction of the PP cross-section surface area and its substitution by the rigid ash particles unable to elongate, as well as the presence of big particles, act as stress raisers and failure points. All these factors, in addition to the improved interfacial adhesion between ash and PP promoted by MAPP, have a concomitant negative effect on the material ductility, independently of ash content.

3.2. Fracture behavior under quasi-static loading conditions

Fig. 2a and b presents typical load–displacement records obtained in three-point-bending tests on SENB specimens under quasi-static loading conditions for the PP matrix and the composites without and with MAPP, respectively. Irrespective of the ash content used, all materials displayed non-linear load–displacement behavior with stable crack growth. In addition, fracture surfaces were found to be highly stress-whitened (Fig. 3).

According to Linear Elastic Fracture Mechanics, for valid plane strain fracture toughness determinations linear-elastic behavior up to the point of fracture and plane strain conditions are simultaneously required. Although these requirements were not satisfied in our experiments, K_{IQ} and G_{IQ} values still reflect a critical state for crack initiation [25] and hence, they were used here to compare

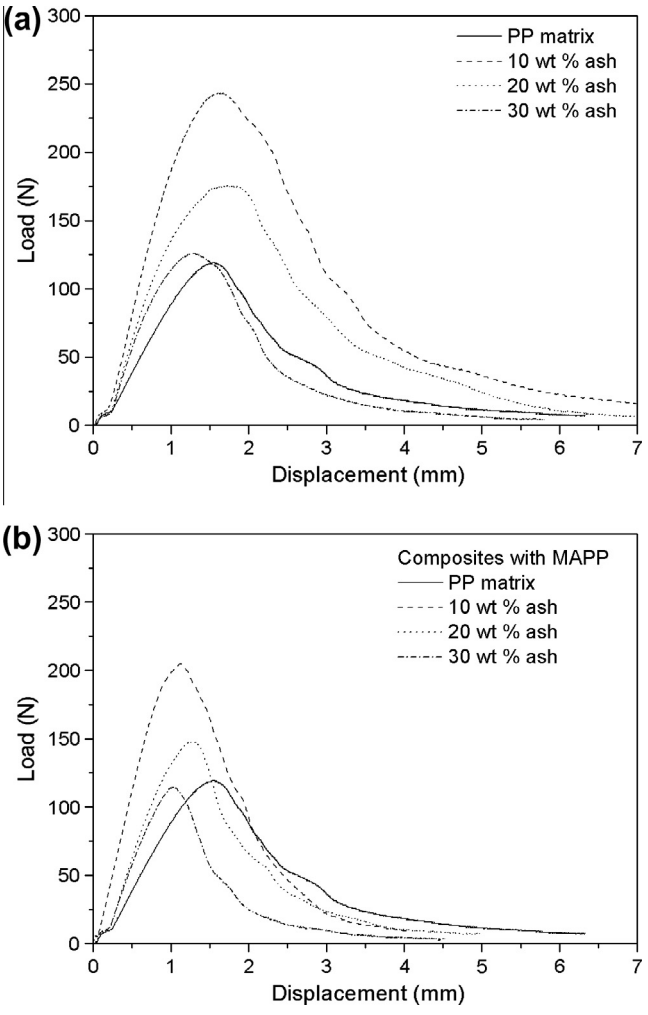

Fig. 2. Typical load–displacement records obtained under quasi-static loading conditions for the different composites investigated. (a) Composites without MAPP. (b) Composites with MAPP.

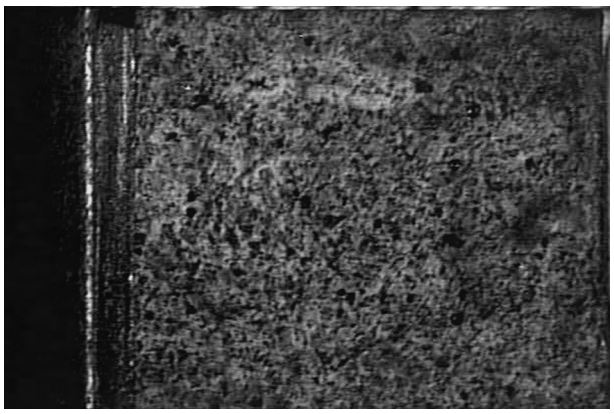

Fig. 3. Optical micrograph of the fracture surface of a SENB sample fractured under quasi-static loading conditions. (Crack propagated from the left to the right).

the resistance of the materials to crack initiation. The results are shown in Table 2.

As it can be seen in this table, the presence of ash led to improved fracture properties with respect to the matrix. It has been shown in a previous investigation [12] that this improvement arises from the development of the toughening mechanisms of particle debonding and subsequent matrix ductile tearing induced by the presence of ash particles. However, the incorporation of MAPP in the composites formulation led to reduced fracture toughness values which, in the case of the energy release rate, were even lower than those of the matrix and were much lesser dependent on ash content. This result suggests that the increased adhesion between ash and PP achieved from the addition of MAPP which will be shown later, hindered the toughening mechanisms induced by the ash particles independently of ash content.

Fig. 4a and b shows SEM micrographs of the fracture surfaces of the composites with 20 wt% ash without and with MAPP, respectively as an example. It is clearly observed in these figures that ash particles debonded from the PP matrix which underwent ductile tearing around these particles. However, by comparing Fig. 4a and b it can be seen that the composites with MAPP exhibited a lower degree of ductile tearing of the matrix material as PP fibrils appear shorter in Fig. 4b. This is in agreement with the important decrease in toughness observed for PP/MAPP/ash composites respect to the composites without coupling agent.

Fig. 5 is a closer view of Fig. 4a in the zone around an ash particle which debonded from the PP matrix. Plastic void growth and ductile tearing of the matrix material are clearly seen in this figure. The cenosphere morphology of fly ash consisting in a hollow particle with porosity in the center and in the walls [26,27] is also observed in Fig. 5.

Table 2
Fracture parameters for the different composites investigated.

Ash content (wt%)	Quasi-static critical stress intensity factor, K_{IQ} (MPa m$^{1/2}$)	Quasi-static critical energy release rate, G_{IQ} (KJ/m^2)	Impact critical energy release rate, G_{IC} (KJ/m^2)
PP/ash composites			
0	1.31 ± 0.15	3.66 ± 0.40	1.30 ± 0.13
10	2.54 ± 0.45	7.26 ± 1.36	1.82 ± 0.24
20	2.05 ± 0.40	5.84 ± 0.68	3.04 ± 0.67
30	1.67 ± 0.23	4.48 ± 0.22	2.27 ± 0.88
PP/MAPP/ash composites			
10	2.07 ± 0.15	3.80 ± 0.38	1.74 ± 0.03
20	1.57 ± 0.26	3.08 ± 0.42	2.06 ± 0.16
30	1.33 ± 0.11	2.32 ± 0.17	1.60 ± 0.16

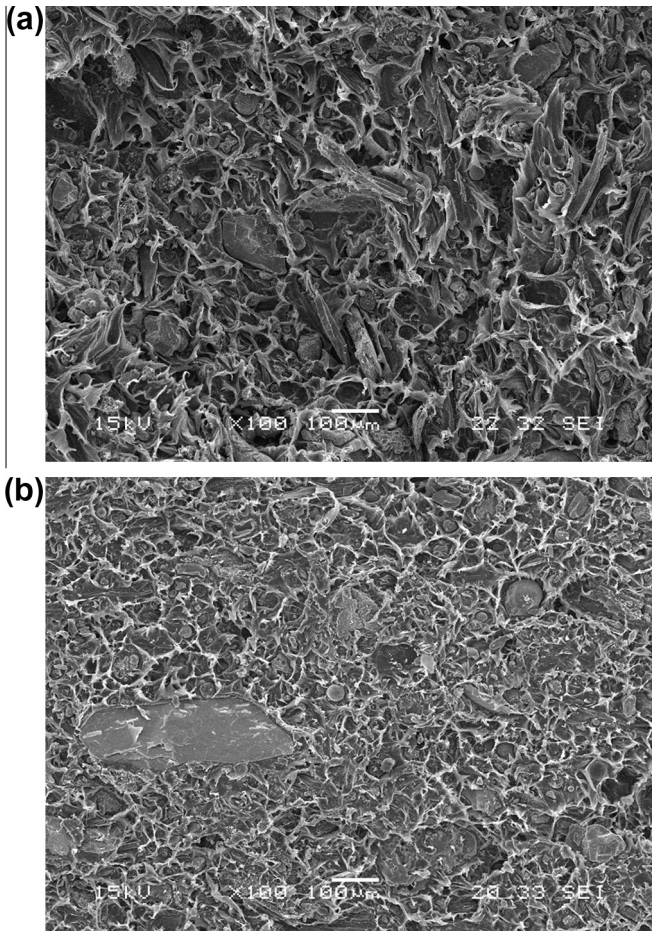

Fig. 4. SEM fractographs of SENB samples tested under quasi-static loading conditions. (a) PP/ash composite with 20 wt% ash. (b) PP/MAPP/ash composite with 20 wt% ash.

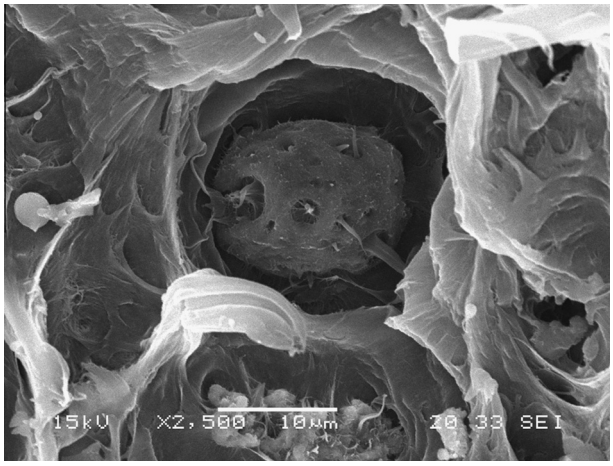

Fig. 5. Closer view of Fig. 4a.

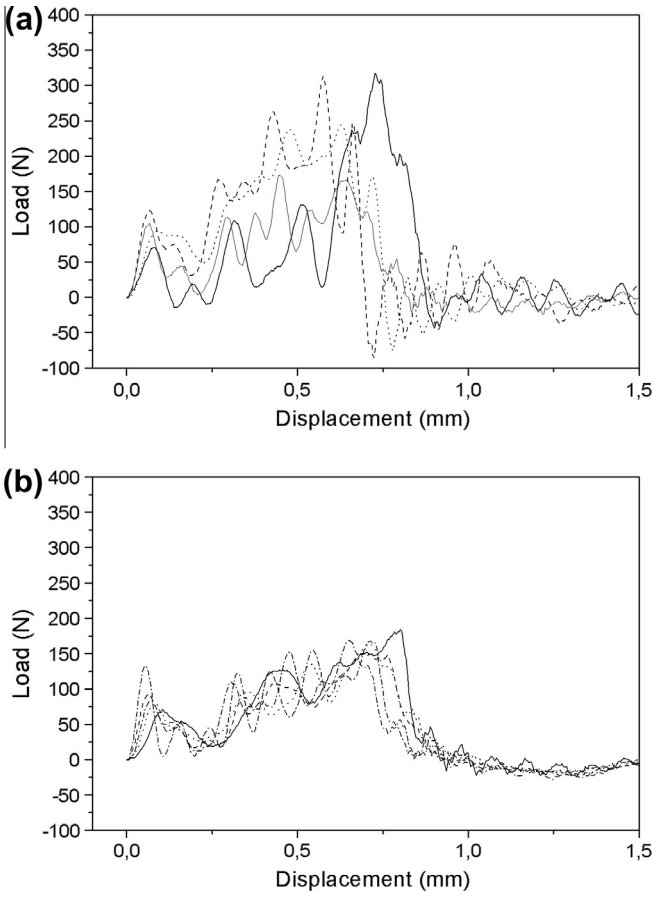

Fig. 6. Typical load–displacement records obtained under impact loading conditions for the different composites investigated. (a) PP/ash composite with 20 wt% ash. (b) PP/MAPP/ash composite with 20 wt% ash.

3.3. Fracture behavior under impact loading conditions

Fig. 6a and b shows force–displacement records obtained on SENB specimens under impact loading conditions for the composite with 20 wt% ash without and with MAPP, respectively as an example. Fully brittle behavior was exhibited for all materials, irrespectively of ash content. Under impact loading, plastic deformation of the matrix is suppressed by the high strain rate as well as the constraint imposed by the rigid filler. In addition, the material in front of the crack tip is subjected to plane-strain conditions and the crack propagates through the matrix with little or no plastic deformation [28]. It should also be noted that the addition of MAPP in the formulation led to more repetitive records (compare Fig. 6a and b), suggesting improved dispersion of ash particles in the PP matrix in agreement with Young's modulus results.

Macroscopically, fracture surfaces of samples broken in impact fracture tests did not exhibit stress whitening (Fig. 7) confirming the absence of the matrix plastic deformation and being in agreement with the fully brittle load–displacement records observed.

For all composites, critical initiation energy release rate values obtained in impact were higher than those of PP (Table 2) and they also displayed a maximum at about 20 wt% ash. The important decrease of the scatter of experimental data for PP/MAPP/ash composites is also evident in this figure.

Furthermore, in agreement with tensile and quasi-static fracture results, the presence of MAPP in the composites formulation has a detrimental effect on the materials impact fracture behavior. A negative effect of MAPP on impact strength has been also reported by others [25].

Fig. 8 shows SEM micrographs of fracture surfaces of 20 wt% ash composite samples broken in impact tests without and with MAPP respectively, as an example. No signs of fibrils of PP indicative of the matrix ductile tearing were observed, in agreement with macroscopic observations, thus confirming that the amount of plastic deformation on the fracture plane is rather limited. Therefore, a

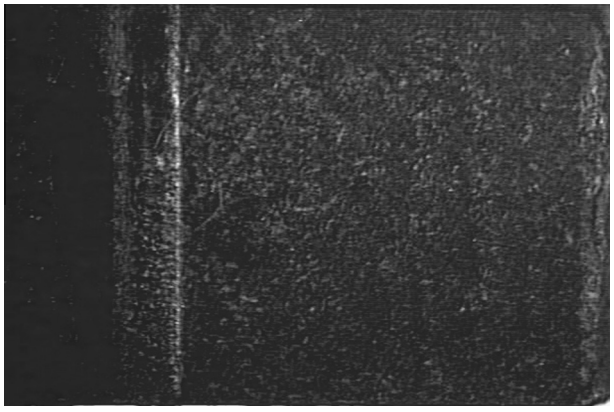

Fig. 7. Optical micrograph of the fracture surface of a SENB sample fractured under impact loading conditions. (Crack propagated from the left to the right).

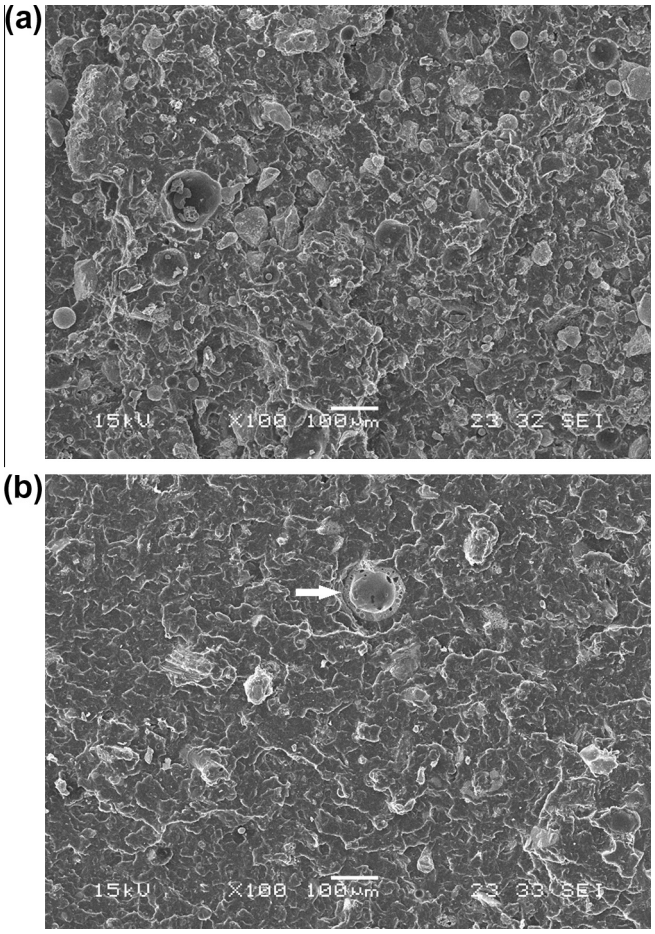

Fig. 8. SEM fractographs of SENB samples tested under impact loading conditions. (a) PP/ash composite with 20 wt% ash. (b) PP/MAPP/ash composite with 20 wt% ash.

small amount of energy was dissipated within the damage zone and hence, the measured toughness was low (impact fracture energy values were significantly lower than quasi-static values) [29].

It can also be observed in Fig. 8a, that many particles are present on the fracture surface of the PP/ash composites without coupling agent. Most of these particles are nearly clean, suggesting that during crack propagation, the fracture front preferentially passed from the interface rather than going through ash particles. This indicates a rather poor adhesion between ash and PP.

On the other hand, the incorporation of MAPP in the composites formulation, led to a more homogeneous dispersion of ash particles in the PP matrix and also improved interfacial adhesion between ash and PP, as ash particles in Fig. 8b are not as distinguishable as particles in Fig. 8a. Moreover, a broken ash particle can also be observed in Fig. 8b as a result of the greater interfacial adhesion.

The presence of maleated PP [28] is expected to greatly improve interfacial adhesion contributing to the formation of a strong interfacial layer that alters the local stress distribution and hence, changing the deformation and fracture mechanisms. It is believed that the maleic anhydride groups of MAPP are able to react with the surface hydroxyl groups of ash particles. Therefore, maleic anhydride which is a rigid five-membered ring with a permanent dipole moment is expected to act as a coupling agent, breaking up agglomerates and increasing the degree of particles dispersion in the matrix and interfacial adhesion between both phases [24]. The Polypropylene segments of MAPP formed miscible blends with the bulk PP through cocrystallization, and the polar part of MAPP formed a chemical bond with ash, or a polar filler in general. The surface hydroxyl groups of ash particles react as a nucleophile with the maleic anhydride groups of the grafting agent. The mechanism of maleic anhydride (MAPP) is schemed in Fig. 9.

In our case, the high surface roughness of ash would have also contributed to the strong interaction offering sites for mechanical anchoring.

Due to reactions taking place between hydroxyl groups of the filler and maleic anhydride groups of copolymer [24], as well as the mechanical anchoring mentioned above, the formation of a strong bonding between ash particles and PP macromolecules was achieved. Therefore, the interface became more rigid and particle debonding from the matrix was hindered. As a result, fracture toughness, especially under impact loading conditions, was greatly reduced from the incorporation of MAPP.

3.4. Crystallization behavior and their relationship with tensile and fracture behavior

The behavior of PP based composites in engineering applications critically depends on the extent of crystallinity and the nature of the crystalline morphology of PP [1,30]. Considering that, crystallization temperature (T_c), melting temperature (T_m) and degree of crystallinity were evaluated for neat PP, PP/MAPP blend and composites with and without MAPP, using DSC. Results are shown in Table 3 along with their deviations. The presence of MAPP in composites formulation was previously reported to change the crystallization behavior of PP leading to a decrease in the crystallinity and hence, in the matrix stiffness [31]. The decrease in the regularity of the chains as a result of the modification by maleic anhydride units led in that case to reduced crystallization tendency (decreased crystallinity and melting point) [32–35].

However, in our case it can be inferred from the obtained results that there is not a clear influence of MAPP over the crystallization process. Composites with and without coupling agent exhibit similar values of T_c, T_m and x_c. On the other side, ash particles are expected to act as nucleating agents making the spherulite size decrease and the crystallinity increase [36]. Thermal analysis by DSC made for similar PP/ash composites [14] has shown that T_c and degree of crystallinity of PP increase with ash content, suggesting that PP crystallization starts earlier and ash acts as nucleating agent [37] This expected behavior was also observed in our systems concerning crystallization temperature: an increase in T_c in the composites prepared using both neat PP or MAPP modified PP as matrix.

The maximum in the impact critical energy release rate observed for our composites with 20 wt% ash, can be related to the crystallinity of PP. A maximum in impact strength has been

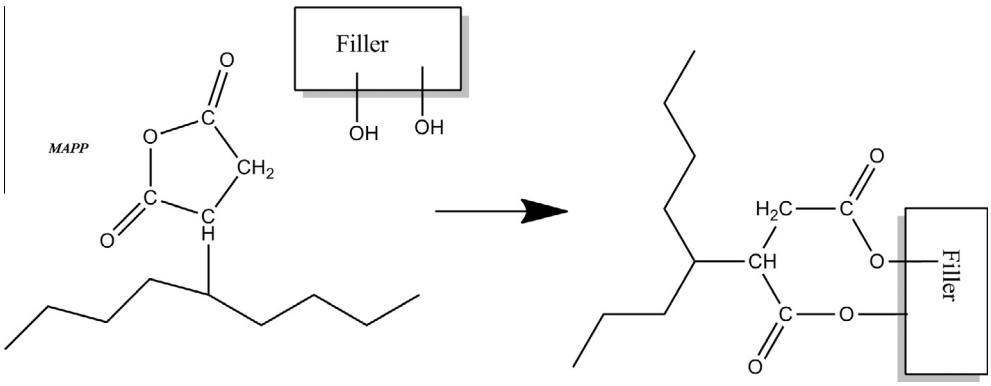

Fig. 9. Schematic representation of the mechanism of maleic anhydride (MAPP).

Table 3
Thermal properties for the different PP/ash composites investigated.

Ash content (wt%)	T_c (°C)	T_m (°C)	x_c
PP/ash composites			
0	118.9 ± 0.6	165.7 ± 0.9	0.48 ± 0.04
10	119.9 ± 0.1	166.8 ± 0.1	0.53 ± 0.02
20	120.3 ± 0.4	165.2 ± 0.6	0.49 ± 0.04
30	122.5 ± 0.9	166.3 ± 1.2	0.51 ± 0.07
PP/MAPP/ash composites			
0	119.4 ± 0.3	166.8 ± 1.2	0.51 ± 0.03
10	120.4 ± 0.2	165.2 ± 1.1	0.52 ± 0.05
20	120.4 ± 0.1	166.4 ± 2.7	0.46 ± 0.09
30	121.7 ± 0.5	164.9 ± 0.4	0.51 ± 0.04

previously reported in the literature [38] for PP modified with different contents of an effective nucleating agent. This maximum agrees in our materials with a minimum in the degree of crystallinity for composites containing 20 wt% ash. It is thought that crystallites act as stress concentrators, intensifying the stress locally far above the applied stress and hence, they probably reduce the material susceptibility to multiple crazing and shear yielding [39].

Moreover, XRD analysis developed for PP/ash and PP/MAPP/ash composites (Fig. 10) indicated that there is not any change in the crystalline structure of PP as a consequence of maleinization or reinforcement which could be related to changes in the materials' tensile and/or fracture behavior.

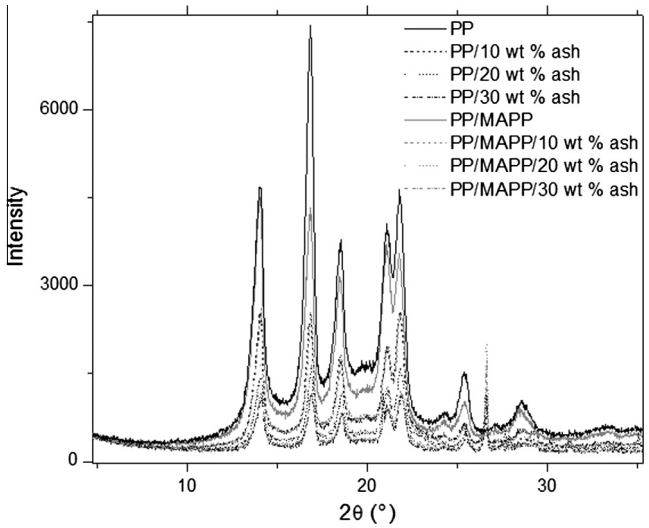

Fig. 10. XRD spectra for the different PP/ash and PP/MAPP/ash composites investigated.

4. Conclusions

The deformation and fracture behavior of PP/ash composites with and without maleic anhydride functionalized iPP (MAPP) as coupling agent was investigated. Especial emphasis was put on the effect of ash content and loading conditions.

Under tension, an increasing trend of stiffness with ash content was found for all composites, whereas a significant reduction in both tensile strength and strain at break values was observed with filler loading for the composites without MAPP as a result of debonding of ash particles from the PP matrix. In contrast, tensile strength and elongation at break for the PP/MAPP/ash composites were roughly independent of ash content.

Under quasi-static loading conditions, improved fracture properties respect to the matrix were observed for the PP/ash composites from the development of the toughening mechanisms of particle debonding and subsequent matrix ductile tearing, induced by the presence of ash particles as observed in SEM fractographs. However, the incorporation of MAPP led to reduced fracture toughness values which, in the case of the energy release rate, were even lower than those of the matrix and were much lesser dependent on ash content. This result suggests that the increased adhesion between ash and PP achieved from the addition of MAPP (revealed from SEM analysis), hindered the toughening mechanisms induced by the ash particles independently of ash content.

Impact critical initiation energy release rate values of the composites were higher than those of PP and they also displayed a maximum at about 20 wt% ash. This maximum was explained in terms of the comprehensive analysis of the crystallinity development in PP. Furthermore, in agreement with tensile and quasi-static fracture results, the presence of MAPP in the composites formulation has also a detrimental effect on the materials impact fracture behavior.

The incorporation of MAPP in the composites formulation also led to better dispersion of ash particles in the PP matrix as revealed from the results of Young's modulus and impact fracture toughness and from SEM observations.

From the results of this investigation, it can be concluded that because composites properties strongly depend on the degree of crystallinity as well as on interfacial adhesion between phases, the relative importance of these effects is difficult to predict and therefore, the composites mechanical behavior (especially fracture behavior) cannot be easily determined in advance.

Acknowledgement

The authors want to thank the National Research Council of Argentina (CONICET) for financial support of this investigation.

References

[1] Greco A, Musardo A, Maffezzoli A. Flexural creep behaviour of PP matrix woven composite. Compos Sci Technol 2007;67:1148–58.
[2] Rohlmann CO, Failla MD, Quinzani LM. Linear viscoelasticity and structure of polypropylene/montmorillonite nanocomposites. Polymer 2006;47:7795–804.
[3] Papgeorgiou D, Bikiaris D, Chrissafis K. Effect of crystalline structure of polypropylene random copolymers on mechanical properties and thermal degradation kinetics. Thermochim Acta 2012;543:288–94.
[4] Aurrekoetxea J, Sarrionandia M, Mateos M, Aretxabale L. Repeated low energy impact behaviour of self-reinforced polypropylene composites. Polym Test 2011;30:216–21.
[5] Esposito Corcione C, Prinari P, Cannoletta D, Mensitieri G, Maffezzoli A. Synthesis and characterization of clay-nanocomposite solvent-based polyurethane adhesives. Int J Adhes Adhes 2008;28:91–100.
[6] Alexandre M, Dubois P. Polymer-layered silicate nanocomposites: preparation, properties and uses of a new class of materials. Mater Sci Eng: Reports 2000;28:1–63.
[7] Manias E, Touny A, Wu L, Strawhecker K, Lu B, Chung TC. Polypropylene/montmorillonite nanocomposites. Review of the synthetic routes and materials properties. Chem Mater 2001;13:3516–23.
[8] Paul DR, Robeson LM. Polymer nanotechnology: nanocomposites. Polymer 2008;49:3187–204.
[9] Zhang YQ, Lee JH, Rhee JM, Rhee KY. Polypropylene–clay nanocomposites prepared by in situ grafting–intercalating in melt. Compos Sci Technol 2004;64:1383–9.
[10] Krawczak P. Compounding and processing of polymer nanocomposites: from scientific challenges to industrial stakes. Express Poly Lett 2007;1:188.
[11] Nath DCD, Bandyopadhyay S, Yu A, Zeng Q, Das T, Blackburn D, et al. Structure–property interface correlation of fly ash-isotactic polypropylene composites. J Mater Sci 2009;44:6078–89.
[12] Pardo SG, Bernal C, Abad MJ, Cano J, Barral Losada L. Deformation and fracture behavior of PP/ash composites. Compos Interfaces 2009;16:97–114 [Special Issue].
[13] Pardo SG, Bernal C, Abad MJ, Cano J. Rheological, thermal and mechanical characterization of fly ash-thermoplastic composites with different coupling agents. Polym Compos 2010;31:1722–30.
[14] Pardo SG, Bernal C, Abad MJ, Cano J, Ares A. Fracture and thermal behaviour of biomass ash polypropylene composites. J Thermoplast Compos Mater 2013. http://dx.doi.org/10.1177/0892705712452740.
[15] Móczó J, Pukánszky B. Polymer micro and nanocomposites: structure, interactions, properties. J Ind Eng Chem 2008;14:535–63.
[16] Fu S-Y, Feng X-Q, Lauke B, Mai Y-W. Effects of particle size, particle/matrix interface adhesion and particle loading on mechanical properties of particulate–polymer composites. Composites: Part B 2008;39:933–61.
[17] Pionteck J, Sadhu VB, Jakisch L, Pötschke P, Häubler L, Janke A. Crosslinkable coupling agents: synthesis and use for modification of interfaces in polymer blends. Polymer 2005;46:6563–74.
[18] Thongsang S, Sombatsompop N. Effect of NaOH and Si69 treatments on the properties of fly ash/natural rubber composites. Polym Compos 2005;27:30–40.
[19] Karger-Kocsis J. In: Paul DR, Bucknall CB, editors. Reinforced polymer blends, in polymer blends: performance, vol. 2. New York: Wiley; 2000.
[20] Ayswarya EP, Vidya FKF, Renju VS, Eby TT. Rice husk ash – a valuable reinforcement for high density polyethylene. Mater Des 2012;41:1–7.
[21] ISO 17281. Plastics, Determination of fracture toughness (GIC and KIC) at moderately high loading rates (1 m/s); 2002.
[22] Brandrup J, Immergut EH. Polymer handbook. New York: Wiley; 1999.
[23] Wong S-C, Mai Y-W. Effect of rubber functionality on microstructures and fracture toughness of impact-modified nylon 6, 6/polypropylene blends: 1. Structure–property relationships. Polymer 1999;40:1553–66.
[24] Bikiaris DN, Vassillou A, Pavlidou E, Karayannidis GP. Compatibilisation effect of PP-g-MA copolymer on iPP/SiO_2 nanocomposites prepared by melt mixing. Eur Polym J 2005;41:1965–78.
[25] Gensler R, Plummer CJG, Grein G, Kausch HH. Influence of the loading rate on the fracture resistance of isotactic polypropylene and impact modified isotactic polypropylene. Polymer 2000;41:3809–19.
[26] Stocchi A, Rodríguez E, Vázquez A, Bernal C. Deformation and fracture behavior of vinylester/fly ash composites. J Appl Polym Sci 2013. http://dx.doi.org/10.1002/app.38305.
[27] Matsunaga T, Kim JK, Hardcastle S, Rohatgi PK. Crystallinity and selected properties of fly ash particles. Mater Sci Eng 2002;325:333–43.
[28] Hristov VN, Lach R, Grellmann W. Impact fracture behavior of modified polypropylene/wood fiber composites. Polym Test 2004;23:581–9.
[29] Zebarjad SM, Lazzeri A, Bagheri R, Seyed Reihani SM, Frounchi M. Fracture mechanism under dynamic loading of elastomer-modified polypropylene. Mater Lett 2003;57:2733–41.
[30] Xu W, Liang G, Zhai H, Tang S, Hang G, Pan W-P. Preparation and crystallization behaviour of PP/PP-g-MAH/Org-MMT nanocomposite. Eur Polym J 2003;39:1467–74.
[31] Kim D, Fasulo PD, Rodgers WR, Paul DR. Structure and properties of polypropylene-based nanocomposites: effect of PP-< i> g</i>-MA to organoclay ratio. Polymer 2007;48:5308–23.
[32] Menyhárd A, Varga J. The effect of compatibilizers on the crystallisation, melting and polymorphic composition of β-nucleated isotactic polypropylene and polyamide 6 blends. Eur Polym J 2006;42:3257–68.
[33] Seo Y, Kim J, Kim KU, Kim YC. Study of the crystallization behaviors of polypropylene and maleic anhydride grafted polypropylene. Polymer 2000;41:2639–46.
[34] Cho K, Li F, Choi J. Crystallization and melting behavior of polypropylene and maleated polypropylene blends. Polymer 1999;40:1719–28.
[35] Li J, Zhou C, Gang W. Study on nonisothermal crystallization of maleic anhydride grafted polypropylene/montmorillonite nanocomposite. Polym Test 2003;22:217–23.
[36] Yu J, He J. Crystallization kinetics of maleic anhydride grafted polypropylene ionomers. Polymer 2000;41:891–8.
[37] Bartczak Z, Argon AS, Cohen RE, Weinberg M. Toughness mechanism in semi-crystalline polymer blends: II. High-density polyethylene toughened with calcium carbonate filler particles. Polymer 1999;40:2347–65.
[38] Xu T, Yu J, Jin Z. Effects of crystalline morphology on the impact behavior of polypropylene. Mater Des 2001;22:27–31.
[39] Galeski A. Strength and toughness of crystalline polymer systems. Prog Polym Sci 2003;28:1646–99.